RNA-Seq Links the Transcription Factors AINTEGUMENTA and AINTEGUMENTA-LIKE6 to Cell Wall Remodeling and Plant Defense Pathways[1][OPEN]

Beth A. Krizek*, Carlton J. Bequette, Kaimei Xu, Ivory C. Blakley, Zheng Qing Fu, Johannes W. Stratmann, and Ann E. Loraine*

Department of Biological Sciences, University of South Carolina, Columbia, South Carolina (B.A.K., C.J.B., K.X., Z.Q.F., J.W.S.); and Department of Bioinformatics and Genomics, University of North Carolina, Charlotte, North Carolina (I.C.B., A.E.L.)

ORCID IDs: 0000-0001-5821-0180 (B.A.K.); 0000-0002-5468-0721 (K.X.); 0000-0003-4532-6453 (I.C.B.); 0000-0002-5673-9272 (J.W.S.).

AINTEGUMENTA (ANT) and AINTEGUMENTA-LIKE6 (AIL6) are two related transcription factors in Arabidopsis (*Arabidopsis thaliana*) that have partially overlapping roles in several aspects of flower development, including floral organ initiation, identity specification, growth, and patterning. To better understand the biological processes regulated by these two transcription factors, we performed RNA sequencing (RNA-Seq) on *ant ail6* double mutants. We identified thousands of genes that are differentially expressed in the double mutant compared with the wild type. Analyses of these genes suggest that ANT and AIL6 regulate floral organ initiation and growth through modifications to the cell wall polysaccharide pectin. We found reduced levels of demethylesterified homogalacturonan and altered patterns of auxin accumulation in early stages of *ant ail6* flower development. The RNA-Seq experiment also revealed cross-regulation of *AIL* gene expression at the transcriptional level. The presence of a number of overrepresented Gene Ontology terms related to plant defense in the set of genes differentially expressed in *ant ail6* suggest that ANT and AIL6 also regulate plant defense pathways. Furthermore, we found that *ant ail6* plants have elevated levels of two defense hormones: salicylic acid and jasmonic acid, and show increased resistance to the bacterial pathogen *Pseudomonas syringae*. These results suggest that ANT and AIL6 regulate biological pathways that are critical for both development and defense.

Flowers initiate on the flanks of the inflorescence meristem, a dome-shaped structure at the apex of a plant. After outgrowth of a flower primordium from the meristem, floral organ primordia appear in characteristic positions within the flower and undergo coordinated cellular behaviors and morphogenesis to develop into one of four organ types. A large number of proteins regulating flower development have been identified in the model plant Arabidopsis (*Arabidopsis thaliana*; for review, see Ó'Maoiléidigh et al., 2014). While certain aspects of flower development, such as the specification of floral organ identity, are well characterized, other aspects remain less well understood. For example, we know little about the molecular mechanisms regulating floral organ initiation, those controlling floral organ size, or those coordinating growth, differentiation, and patterning during floral organogenesis. Four members of the AINTEGUMENTA-LIKE (AIL) transcription factor family, AINTEGUMENTA (ANT), AIL5, AIL6, and AIL7, have partially overlapping roles in some of these less well-understood processes and are required for the establishment of floral organ identity (Krizek, 2009, 2015) Within the AIL family, ANT and AIL6 make the most significant contributions to flower development, acting early to promote flower primordium initiation and later to direct several aspects of floral organ development (Krizek, 2009; Yamaguchi et al., 2013).

Auxin maxima in the periphery of the inflorescence meristem are created through local auxin biosynthesis as well as polar transport of the hormone through the auxin efflux carrier, PIN-FORMED1 (PIN1; Gälweiler et al., 1998; Benková et al., 2003; Reinhardt et al., 2003; Heisler et al., 2005; Cheng et al., 2006). Flower primordium initiation is mediated by the transcription factor MONOPTEROS (MP)/AUXIN RESPONSE FACTOR5

[1] This work was supported by the National Institutes of Health (INBRE Bioinformatics Pilot Project grant to B.A.K.) and the National Science Foundation (grant no. IOS 1354452 to B.A.K. and A.E.L. and grant nos. DBI–0421683 and RCN 009281 for distribution of the JIM5 antibody).

* Address correspondence to krizek@sc.edu and ann.loraine@uncc.edu.

The author responsible for distribution of materials integral to the findings presented in this article in accordance with the policy described in the Instructions for Authors (www.plantphysiol.org) is: Beth A. Krizek (krizek@sc.edu).

B.A.K. and A.E.L. designed the research; B.A.K. prepared the samples for RNA-Seq and performed RT-qPCR, immunolocalization, and confocal microscopy; C.J.B. performed the SA and JA measurements; K.X. performed the bacterial growth assay; I.C.B. and A.E.L. performed bioinformatic data processing and analyses; Z.Q.F. supervised the bacterial growth assay; B.A.K., Z.Q.F., J.W.S., and A.E.L. interpreted the data; B.A.K. and A.E.L. wrote the article; all authors revised and approved the final article.

[OPEN] Articles can be viewed without a subscription.

www.plantphysiol.org/cgi/doi/10.1104/pp.15.01625

(Przemeck et al., 1996). MP activates the floral meristem identity factor LEAFY (LFY) as well as ANT and AIL6 to promote flower primordium initiation (Yamaguchi et al., 2013). Within the flower primordium, sites of floral organ initiation also are correlated with sites of auxin accumulation (Chandler et al., 2011). It is not clear whether auxin specifies the cells that will give rise to floral organ primordia or accumulates in these cells after their specification. Furthermore, it is not known how auxin mediates floral organ outgrowth. After the initiation of floral organ primordia, these primordia adopt fates as sepals, petals, stamens, or carpels in response to distinct combinations of floral organ identity gene activities as described in the ABCE model (for review, see Krizek and Fletcher, 2005). The floral organ identity genes encode transcription factors that regulate target genes throughout floral organ development to bring about the elaboration of characteristic floral organ forms (Ito et al., 2004, 2007; Kaufmann et al., 2010; Wuest et al., 2012; Ó'Maoiléidigh et al., 2013).

ANT and AIL6 are key regulators of several aspects of floral organogenesis, including floral organ initiation, identity specification, growth, and patterning (Krizek, 2009). Flowers that form in *ant ail6* double mutants are composed of fewer and smaller floral organs that arise in relatively random positions within the flower primordia. In addition, these flowers lack petals and normal stamens and carpels; they consist primarily of sepals, some staminoid organs, unfused carpel valves, and organs not present in normal flowers. Despite the importance of ANT and AIL6 in flower development, few regulatory targets of these transcription factors have been identified, and little is known about the biological and cellular means by which they promote growth and development. Previous work has suggested that ANT may regulate organ growth by controlling the length of a cell division-competent state within developing lateral organs (Mizukami and Fischer, 2000). The larger leaves of *35S:ANT* plants are associated with prolonged expression of *CycD3* and a longer period of growth, suggesting that ANT might regulate the expression of cell cycle genes. However, ANT does not appear to regulate *CycD3* expression in petals (Randall et al., 2015).

Thus, to gain insight into the biological roles of ANT and AIL6 in flower development, we used a transcriptomic approach to identify genes that are differentially expressed in *ant ail6* inflorescences. Our results link ANT and AIL6 function in floral organ initiation to changes in the cell wall polysaccharide pectin. Unexpectedly, we also identify roles for ANT and AIL6 in plant defense pathways.

RESULTS

RNA Sequencing of Wild-Type and *ant ail6* Inflorescences

RNA sequencing (RNA-Seq) libraries were constructed from four biological replicates of wild-type (Landsberg *erecta* [Ler]) and *ant-4 ail6-2* inflorescences (Fig. 1, A and B). Reads that mapped uniquely to the genome were used to identify genes differentially expressed in *ant ail6* inflorescences compared with L*er*. Using a false discovery rate of less than 10^{-5} to define differential expression, we identified 3,841 genes up-regulated in *ant ail6* inflorescences compared with L*er* and 4,171 genes down-regulated in *ant ail6* inflorescences compared with L*er* (Supplemental Data S1). The large number of genes misregulated in *ant ail6* inflorescences is consistent with the dramatic differences in flower development in the double mutant, including the almost complete loss of some floral organ identities (petals and stamens), severe disruptions in the patterning and specification of tissue types within the carpel, and alterations in floral organ positioning and growth (Fig. 1, A and B; Krizek, 2009).

The set of genes down-regulated in *ant ail6* includes a number of well-characterized floral regulators, including the floral organ identity genes *APETALA3* (*AP3*), *PISTILLATA* (*PI*), *AGAMOUS* (*AG*), *SEPALLATA1* (*SEP1*), and *SEP2*; the floral organ boundary genes *SUPERMAN* (*SUP*) and *RABBIT EARS* (*RBE*); and the trithorax group factor *ULTRAPETALA2* (*ULT2*; Fig. 1C). Other known regulators of petal, stamen, and carpel development, such as *BIG PETALS* (*BPE*), *SPOROCYTELESS* (*SPL*), and *SEEDSTICK* (*STK*), respectively, also were expressed at lower levels in *ant ail6* inflorescences (Fig. 1C). These results are consistent with the loss or alterations of these floral organ types. Two of the above genes, *AP3* and *AG*, had been shown previously to be expressed at lower levels in *ant ail6* inflorescences (Krizek, 2009). To further validate our results, we performed reverse transcription-quantitative PCR (RT-qPCR) on 11 of the identified genes using an independent set of three biological replicates of L*er* and *ant ail6* inflorescences different from those used to synthesize libraries for RNA-Seq. We found good correlation between the results obtained by RNA-Seq and RT-qPCR (Supplemental Fig. S1).

Functional Categorization of Differentially Expressed Genes

To gain a global view of the gene expression changes occurring in *ant ail6* inflorescences, we performed a Gene Ontology (GO) enrichment analysis on genes identified as being differentially expressed. These analyses identified more than 70 enriched GO terms (Fig. 2; Supplemental Data S2 and S3). The most significantly enriched GO term was plant-type cell wall modification (GO:0009827; Fig. 2). Of the 171 total genes in this GO category, 156 were differentially expressed in *ant ail6* inflorescences, with 153 down-regulated in the double mutant (Supplemental Data S2). Other GO terms that consisted primarily of genes down-regulated in *ant ail6* were related to pollen development, including pollen tube growth (GO:0009860), pollen exine formation (GO:0010584), pollen tube development (GO:0048868), and pollen tube (GO:0090406). These results are consistent with the absence of pollen in *ant ail6* flowers. Although some stamen-like organs are

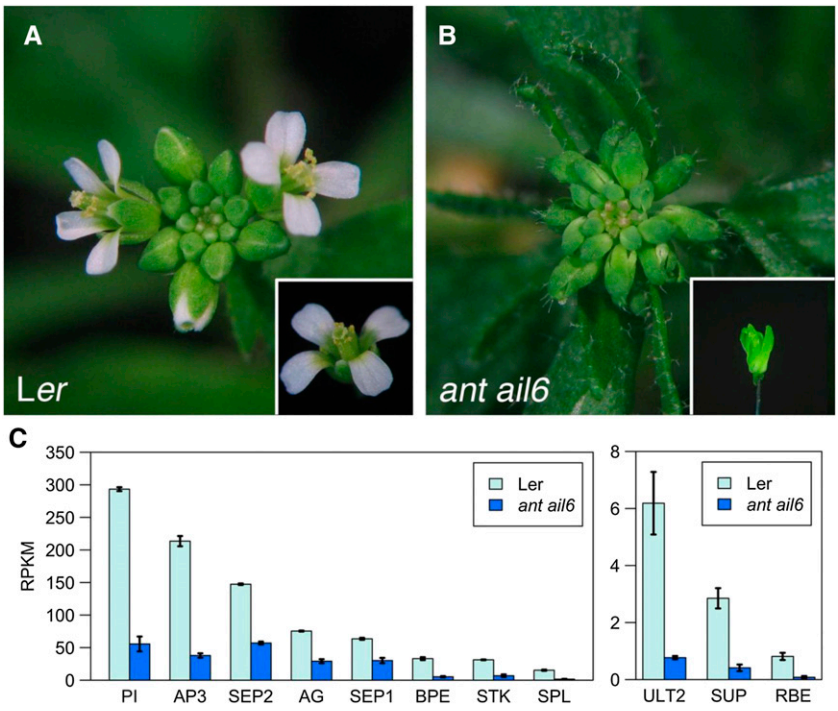

Figure 1. Many known floral regulators are down-regulated in *ant ail6* inflorescences. A, L*er* inflorescence. The inset shows an individual L*er* flower. B, *ant ail6* inflorescence. The inset shows an individual *ant ail6* flower. C, Graphs showing expression levels in reads per kilobase per million mapped reads (RPKM) for the floral regulatory genes *PI*, *AP3*, *SEP2*, *AG*, *SEP1*, *BPE*, *STK*, *SPL*, *ULT2*, *SUP*, and *RBE*. All of these genes are expressed at lower levels in *ant ail6* inflorescences compared with L*er*.

present in *ant ail6* flowers, these organs do not make pollen. Two other enriched GO terms with the majority of genes down-regulated in *ant ail6* were pectinesterase inhibitor activity (GO:0046910) and sexual reproduction (GO:0019953), while indoleacetic acid biosynthetic process (GO:0009684) contained similar numbers of up- and down-regulated genes.

The remainder of the GO terms corresponded to categories in which most genes were up-regulated, including cell differentiation (GO:0030154), leaf morphogenesis (GO:0009965), and a number of terms associated with photosynthesis, including chloroplast thylakoid membrane (GO:0009535), pentose-phosphate shunt (GO:0006098), thylakoid membrane organization (GO:0010027), photosystem II assembly (GO:0010207), photosynthesis, light reaction (GO:0019684), chlorophyll biosynthetic process (GO:0015995), chloroplast relocation (GO:0009902), photosynthesis (GO:0015979), photosynthetic electron transport in photosystem I (GO:0009773), and chloroplast photosystem II (GO: 0030095). These results suggest that the flat green organs that sometimes develop in *ant ail6* flowers in place of petals and stamens are leaf like in identity and capable of photosynthesis.

Another group of significantly enriched GO terms containing a majority of up-regulated genes are associated with plant defense. These include defense response (GO:0006952), jasmonic acid mediated signaling pathway (GO:0009867), defense response to fungus (GO:0050832), negative regulation of defense response (GO:0031348), regulation of plant-type hypersensitive response (GO:0010363), defense response to bacterium (GO:0042742), systemic acquired resistance, salicylic acid mediated signaling pathway (GO:0009627), salicylic acid biosynthetic process (GO:0009697), regulation of innate immune response (GO:0045088), and regulation of defense response (GO:0031347; Fig. 2). The increased expression of defense response genes in *ant ail6* may be a consequence of sepals making up a larger part of *ant ail6* flowers as compared with wild-type flowers. A recent analysis of publicly available transcriptomic data showed that defense genes are some of the most abundant transcripts in stage 12 to 15 sepals, suggesting that sepals play a key role in pathogen defense of the flower (Ederli et al., 2015). Thus, the increased defense gene expression in *ant ail6* may partly or fully be an indirect effect resulting from changes in floral organ identity present in the double mutant.

ant ail6 Inflorescence Meristems and Young Flowers Show Reduced Levels of Demethylesterified Homogalacturonan

Based on the joint identification of the GO terms plant-type cell wall modification (GO:0009827) and pectinesterase inhibitor activity (GO:0046910), we further investigated the expression of genes encoding enzymes that act on the cell wall polysaccharide pectin within the RNA-Seq data set. Pectins, a heterogenous group of polysaccharides rich in GalUA, are a major component of plant primary cell walls. The most abundant pectic polysaccharide is homogalacturonan (HG), a linear polymer of α-(1-4)-linked D-GalUA that is synthesized in the Golgi and deposited in the cell wall in a highly methylesterified form. This modification neutralizes the sugar acid's carboxyl group, making the pectin less acidic and changing its affinity for water and polar molecules. A number of enzymes within the cell

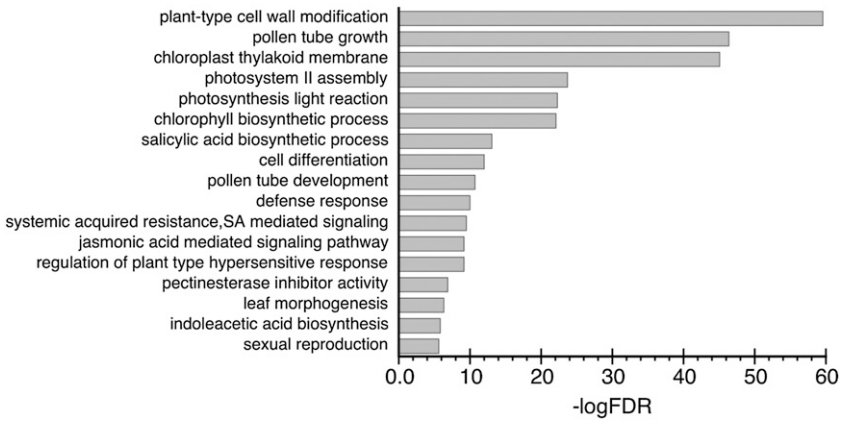

Figure 2. Graph showing a subset of the GO terms significantly enriched in genes differentially expressed in *ant ail6* inflorescences. The most significantly enriched GO term is plant-type cell wall modification. FDR, False discovery rate.

wall act to control the degree of substitution (methylesterification and/or acetylation) as well as the degree of polymerization of pectin (for review, see Sénéchal et al., 2014). Such modifications to pectin affect the rheological properties of the cell wall and, consequently, plant growth and development.

Pectin methylesterases (PMEs) within the cell wall act to demethylesterify HG, while pectin methylesterase inhibitors (PMEIs) regulate PME activity. Demethylesterification of HGs restores the carboxylic acid subgroups on their polygalacturonan subunits, which can result in the formation of egg-box structures in which two HG chains are cross-linked through Ca^{2+} bridges (Grant et al., 1973). Such modifications are thought to result in rigidification of the cell wall. However, demethylesterified HGs also are substrates for enzymes that act to degrade pectin, including polygalacturonases (endo-PGs and exo-PGs) and pectate lyase-like (PLL), and thus ultimately can result in softening of the cell wall. In the inflorescence meristem, demethylesterification of HG promotes cell wall loosening and flower primordium initiation (Peaucelle et al., 2008, 2011). It is not known whether the demethylesterification of HG also may underlie the initiation of floral organs within a flower primordium.

Besides PMEs, PGs, and PLLs, a fourth class of HG-modifying enzymes are pectin acetylesterases (PAEs), which remove acetyl groups that can be present on HG. PMEs, PMEIs, PGs, PLLs, and PAEs all belong to large multigene families (Louvet et al., 2006; Pelloux et al., 2007; Sun and van Nocker, 2010; Cao, 2012; Wang et al., 2013; de Souza et al., 2014). A large number of these HG-modifying enzymes are differentially expressed and primarily down-regulated in *ant ail6* inflorescences, including approximately 58% of PLLs, 55% of PMEIs, 47% of PMEs, and 40% of PGs (Table I; Supplemental Table S1).

We investigated the methylesterification status of HG in *ant ail6* inflorescences using an antibody (JIM5) that binds to sparsely methylesterified HG (Knox et al., 1990). In L*er* inflorescences, we detected low levels of JIM5 signal in the inflorescence meristem and stage 1 to 3 flower primordia (Fig. 3, A and B). Signal was higher in the pedicels of older flowers (Fig. 3, A and B). In a stage 6 L*er* flower, JIM5 signal was strong in the flower pedicel and developing sepals, while little to no signal was visible in the stamen and carpel primordia (Fig. 3C). In *ant ail6* inflorescences, there was overall much lower JIM5 signal throughout the inflorescence apex. No JIM5 signal was visible in *ant ail6* inflorescence meristems or the apex of stage 1 to 3 *ant ail6* flowers (Fig. 3, D–F). Some JIM5 signal was visible in *ant ail6* flower pedicels, but less than that present in L*er* flower pedicels (Fig. 3, A, B, D, and E). In an older *ant ail6* flower, JIM5 signal was observed in developing sepals, but at lower levels compared with L*er* (Fig. 3F). These results indicate that *ant ail6* inflorescence meristems and young flowers exhibit reductions in the levels of demethylesterified HG.

ant ail6 Flowers Exhibit Alterations in Auxin Accumulation Patterns

The identification of the GO term indoleacetic acid biosynthetic process (GO:0009684) led us to further

Table I. *Homogalacturonan-modifying enzymes differentially expressed in ant ail6*

Gene Family	Differential Expression in *ant ail6*/Total	Down-Regulated in *ant ail6*/Total	Up-Regulated in *ant ail6*/Total
PMEs	31/66	25/66	6/66
Group 1	10/21	8/21	2/21
Group 2	21/45	17/45	4/45
PMEIs	39/71	31/71	8/71
PGs	27/68	23/68	4/68
PLLs	15/26	10/26	5/26
PAEs	1/12	1/12	0/12

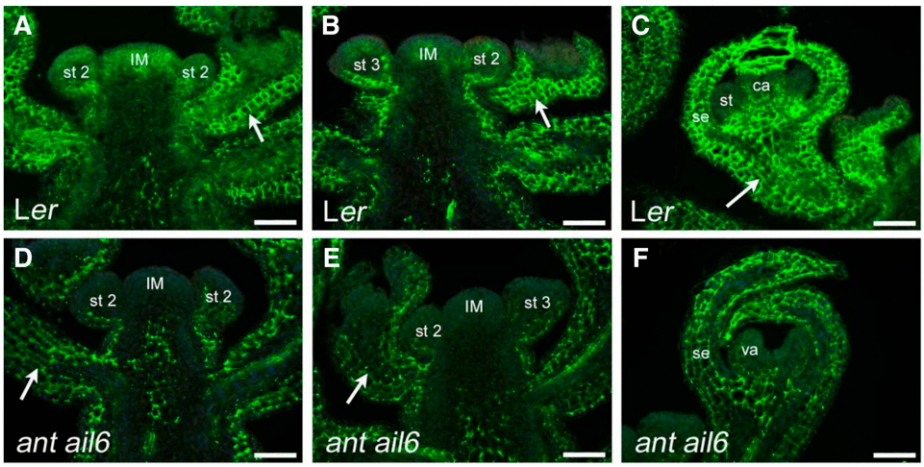

Figure 3. *ant ail6* inflorescences have lower levels of demethylesterified HG. A and B, JIM5 immunolocalization on L*er* inflorescences. Arrows point to flower pedicels. C, JIM5 immunolocalization on a L*er* stage 6 flower. The arrow points to a flower pedicel. D and E, JIM5 immunolocalization on *ant ail6* inflorescences. Arrows point to flower pedicels. There is reduced JIM5 signal in the inflorescence meristem and young flowers compared with L*er*. F, JIM5 immunolocalization on an *ant ail6* flower. ca, Carpel; IM, inflorescence meristem; se, sepal; st, stamen; st 2, stage 2 flower; st 3, stage 3 flower; va, probable carpel valve. Bars = 50 μm.

examine the biosynthetic pathways regulating the production of the auxin indole-3-acetic acid (IAA) using AraCyc (Zhang et al., 2005). Previous work has linked other members of the AIL/PLETHORA family to auxin biosynthesis (Pinon et al., 2013). IAA can be synthesized from L-Trp via a two-step pathway in which L-Trp is converted to indole-3-pyruvic acid by a family of Trp aminotransferases (TAA1) followed by the conversion of indole-3-pyruvic acid to IAA by a family of flavin monooxygenases (YUCCAs [YUCs]; for review, see Brumos et al., 2014). Genes encoding one member of each of these two families, *TAA1* and *YUC2*, show altered expression in *ant ail6* inflorescences, with *TAA1* expressed at lower levels and *YUC2* expressed at higher levels (Fig. 4A). Two additional pathways converting L-Trp to IAA have been proposed to occur in plants, through the intermediates indole-3-acetaldoxime and indole-3-acetamide (Fig. 4A). The expression of several genes encoding enzymes in these putative pathways also is altered in *ant ail6* inflorescences. *CYP79B2* and *CYP79B3*, two genes encoding cytochrome P450 monooxygenases that convert L-Trp to indole-3-acetaldoxime, are down-regulated, while genes encoding later-acting enzymes, such the cytochrome P450 monooxygenase *CYP71A13*, the nitrilase *NIT2*, and the indole-3-acetamide hydrolase *AMI1*, are up-regulated (Fig. 4A). Thus, for all three pathways, the earliest-acting genes are down-regulated in *ant ail6* inflorescences while later-acting genes are up-regulated, making it difficult to predict how these changes might affect auxin levels within the inflorescence.

As auxin may specify the site of floral organ initiation within flower primordia and has been shown to control petal initiation in Arabidopsis (Chandler et al., 2011; Lampugnani et al., 2013), we wondered whether the defects in floral organ initiation in *ant ail6* flowers might result from reduced levels of auxin within young flower primordia. Previous work using the auxin-responsive reporter *AGH3-2*:*GUS* had shown differences in auxin distribution within *ant ail6* flowers (Krizek, 2009). In particular, developing sepals often showed a broader expression of the reporter, with GUS activity detected throughout the organ rather than being restricted to the tips.

To look at earlier stages of flower development with increased spatial resolution, we examined the expression of the auxin-responsive reporter *DR5rev*:*GFP* in L*er* and *ant ail6* inflorescences (Friml et al., 2003). GFP signal accumulates in groups of cells on the periphery of *DR5rev*:*GFP* inflorescences that mark incipient and newly initiated flower primordia (Fig. 4B; Heisler et al., 2005). Within stage 4 flowers, *DR5rev*:*GFP* was detected in discrete foci that correspond to the tips of sepal primordia and sites of petal and stamen initiation (Fig. 4, C and D; Chandler et al., 2011). In *DR5rev*:*GFP ant ail6* inflorescences, we observe a similar accumulation of GFP signal in groups of cells in the periphery of the inflorescence meristem (Fig. 4E). However in stage 4 *DR5rev*:*GFP ant ail6* flowers, we find an increased number of GFP-expressing cells that tend to be present in larger groups, more dispersed throughout the flower primordium, and not present in characteristic positions compared with *DR5rev*:*GFP* primordia (Fig. 4, F and G). In addition, the overall GFP signal is much higher in *DR5rev*:*GFP ant ail6* stage 4 flowers than in *DR5rev*:*GFP* stage 4 flowers (Fig. 4, C–F). Our results show that auxin accumulates to higher overall levels in cells of young *ant ail6* flowers. These cells are more broadly distributed and present at random positions within the flower primordia. Thus, the defects in floral organ initiation in *ant ail6* flowers do not appear to result from reduced levels of auxin.

Cross-Regulation of *AIL* Gene Expression in *ant ail6* Inflorescences

ANT, *AIL6*, and *AIL7* are among the genes up-regulated in *ant ail6* inflorescences. These results were confirmed by RT-qPCR (Fig. 5A) and suggest the cross-regulation of *AIL* expression in the *ant ail6* background. To investigate how general such cross-regulation is within the family, we examined the expression of *ANT*, *AIL5*, *AIL6*, and *AIL7* in *ant* and *ail* single mutants (*ant-4*, *ail5-3*, *ail6-2*, and *ail7-1*) and *ant ail* double mutants (*ant-4 ail5-3*, *ant-4 ail6-2*, and *ant-4*

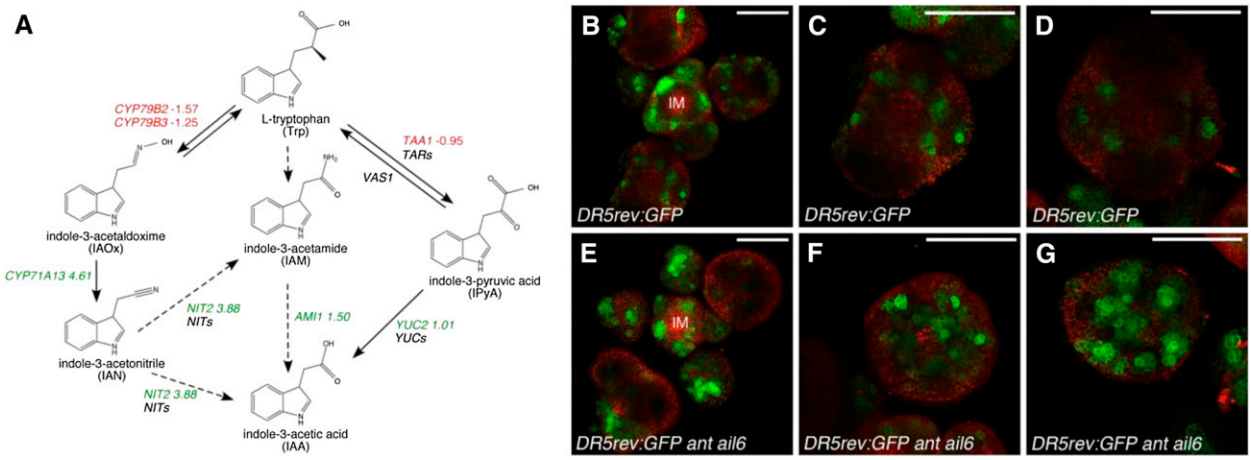

Figure 4. Auxin biosynthesis and distribution in *ant ail6*. A, Characterized and proposed L-Trp-dependent IAA biosynthetic pathways in Arabidopsis. Genes shown in red are down-regulated in *ant ail6* inflorescences, and genes shown in green are up-regulated in *ant ail6* inflorescences. The numbers beside the genes show $\log_2$ fold change. B to G, Top view confocal images of a *DR5rev:GFP* inflorescence meristem (B), *DR5rev:GFP* stage 4 flowers (C and D), *DR5rev:GFP ant ail6* inflorescence meristem (E), and *DR5rev:GFP ant ail6* stage 4 flowers (F and G). The GFP signal is shown in green and the FM4-64 signal in red. IM, Inflorescence meristem. Bars = 50 μm.

ail7-1; Fig. 5A). The *ail5-3* and *ail6-2* transfer DNA alleles are not RNA nulls; partial transcripts of *AIL5* and *AIL6* are detected in the *ail5-3* and *ail6-2* alleles, respectively (Fig. 5A). In contrast, *AIL7* mRNA levels are reduced dramatically in the *ail7-1* transfer DNA insertion allele (Fig. 5A). While the most significant cross-regulation occurs in the *ant ail6* background, the expression of *AIL6* also is elevated slightly in *ant-4*, *ail6-2*, and *ant-4 ail5-3* inflorescences (Fig. 5A). In addition, *ANT* expression is reduced slightly in *ail7-1* and *ant-4 ail7-1* inflorescences, *AIL5* expression is reduced slightly in *ant-4*, *ant-4 ail5-3*, *ail7-1*, and *ant-4 ail7-1* inflorescences, and *AIL7* expression is reduced slightly in *ail5-3* and *ail6-2* inflorescences (Fig. 5A). These results indicate that the functional redundancy of *AIL* genes is accompanied to some degree by the cross-regulation of *AIL* gene expression at the transcriptional level.

To investigate whether the up-regulation of *AIL6* and *AIL7* in *ant ail6* inflorescences resulted from ectopic expression of these genes or higher mRNA levels within the endogenous spatial domain, we performed in situ hybridization. Within the inflorescence meristem, the spatial pattern of *AIL7* mRNA was similar in L*er* and *ant ail6*: strong signal was present in the center of the meristem (Fig. 5, B and C). The distribution of *AIL7* mRNA was sometimes altered in *ant ail6* flowers. In particular, *AIL7* mRNA was missing from the center of some floral meristems in *ant ail6* stage 4 flowers (Fig. 5, D and E). This could be a consequence of these cells losing some stem cell identity as *ant ail6* flowers show premature differentiation of floral meristem cells (Krizek and Eaddy, 2012). Thus, the increased amount of *AIL7* mRNA does not result from ectopic expression but largely from expression at higher levels. We find that this also is true for *AIL6*. *AIL6* shows a similar expression pattern in L*er* and *ant ail6* within the periphery of the inflorescence meristem and developing flowers (Fig. 5, F–I). *AIL6* mRNA also was detected in the procambium of *ant ail6* inflorescences (Fig. 5, F–I). We have observed *AIL6* mRNA in the procambium of wild-type plants previously, although it was not detectable in this experiment, presumably due to the length of time the slides were exposed to substrate (Nole-Wilson et al., 2005).

Cross-regulation of gene expression within gene families that have partial redundancy has been observed previously in Arabidopsis and in some cases involves ectopic expression. Often, ectopic expression of one or several members of a gene family partially compensates for the loss of other members (Vieten et al., 2005; Nimchuk et al., 2015). It is not clear whether increased levels of *AIL7* in *ant ail6* inflorescences may partially compensate for the loss of *ANT* and *AIL6*. Previous work has noted the dose-dependent behavior of *AIL7* in the *ant ail6* double mutant (Krizek, 2015), which indicates that this genetic background is sensitive to *AIL7* levels and suggests that increased expression of *AIL7* could potentially offset the loss of *ANT/AIL6* function to some degree.

ant ail6 Plants Have Higher Salicylic Acid Levels and Show Enhanced Resistance to the Bacterial Pathogen *Pseudomonas syringae*

Identification of the GO terms salicylic acid biosynthetic process (GO:0009697) and systemic acquired resistance, salicylic acid mediated signaling pathway (GO:0009627) led us to further investigate the expression of genes encoding enzymes involved in salicylic acid (SA) accumulation in plants. Although SA biosynthetic pathways have not been fully elucidated, the

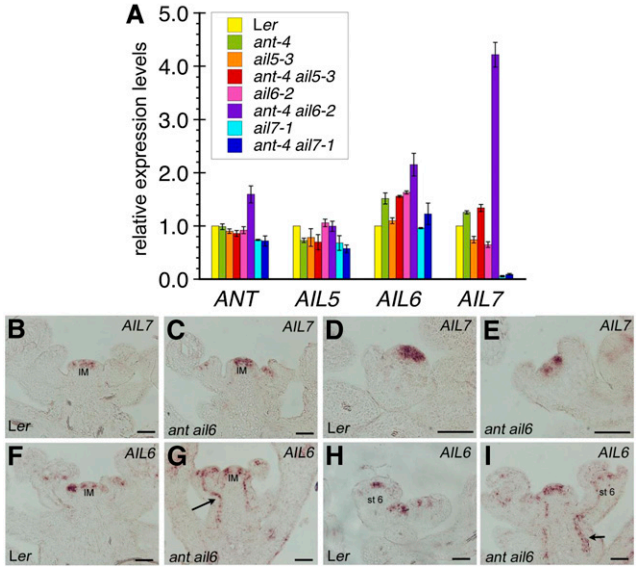

Figure 5. Cross-regulation of *AIL* gene expression. A, RT-qPCR results examining *ANT*, *AIL5*, *AIL6*, and *AIL7* mRNA expression in L*er*, *ant-4*, *ail5-3*, *ant-4 ail5-3*, *ail6-2*, *ant-4 ail6-2*, *ail7-1*, and *ant-4 ail7-1* inflorescences. The expression level in L*er* is set to 1, and error bars show SD. B to E, In situ hybridization of *AIL7* in L*er* and *ant-4 ail6-2*. *AIL7* mRNA expression is shown in L*er* inflorescence (B), *ant-4 ail6-2* inflorescence (C), L*er* stage 4 flower (D), and *ant-4 ail6-2* stage 4 flower (E). F to I, In situ hybridization of *AIL6* in L*er* and *ant-4 ail6-2*. *AIL6* mRNA expression is shown in L*er* inflorescence (F), *ant-4 ail6-2* inflorescence (G), developing L*er* flower (H), and *ant-4 ail6-2* inflorescence (I). Arrows in G and I point to procambium. IM, Inflorescence meristem; st 6, stage 6 flower. Bars = 50 μm.

primary route for stress-induced SA production is the chorismate pathway in chloroplasts (for review, see Dempsey et al., 2011). A second pathway involving Phe appears to play only a minor role. ISOCHORISMATE SYNTHASE1 (ICS1) converts chorismate to isochorismate, which is then converted to SA (Fig. 6A). In *ant ail6* inflorescences, *ICS1* is slightly up-regulated (Fig. 6A). In addition, three activators (WRKY28, SARD1, and CBP60g) of *ICS1* expression are up-regulated in *ant ail6* compared with the wild type (Fig. 6A). After its synthesis, SA can be chemically modified in various ways, including glucosylation, methylation, or conjugation to amino acids; these modifications alter the properties and functions of the hormone. Genes encoding enzymes involved in glucosylation (UGT74F1 and UGT74F2) as well as those involved in methylation (MET2 and MET7) show altered expression in *ant ail6* inflorescences; in each case, one member of the family is up-regulated while a second member is down-regulated (Fig. 6A). To investigate whether the observed expression changes in SA biosynthetic enzymes result in altered levels of the hormone, we measured SA levels in both unwounded and wounded leaves of L*er* and *ant ail6*. We observed higher SA levels in unwounded *ant ail6* leaves compared with unwounded L*er* leaves (Fig. 6B). No significant difference was measured in wounded leaves (Fig. 6B).

In wild-type plants, SA accumulation after pathogen infection contributes to the induction of systemic acquired resistance (SAR; for review, see Fu and Dong, 2013). SAR promotes broad-spectrum resistance in systemic tissues of the plant that protects it for a time against secondary infections. In addition to increased levels of SA, a number of SAR-associated genes are up-regulated in *ant-4 ail6-2* inflorescences (Table II). These include genes for the master regulator of SAR, NONEXPRESSOR OF PR GENES1 (NPR1), TGA transcription factors that interact with NPR1, antimicrobial PATHOGENESIS-RELATED (PR) proteins, and WRKY transcription factors that act downstream of NPR1 (for review, see Fu and Dong, 2013; Table II). These results suggest that SAR is constitutively activated in *ant-4 ail6-2* plants and that these plants might show enhanced resistance to infection with a virulent pathogen. To investigate this possibility, we examined the growth of the bacterial pathogen *P. syringae* pv. *maculicola* 4326 in wild-type and *ant ail6* plants. Three days after infection with *P. syringae*, we found reduced growth of the bacterium and reduced disease symptoms in *ant-4 ail6-2* plants compared with L*er* (Fig. 6, C and D). As a control, we used *npr1-2*, a mutant defective in SAR (Cao et al., 1994). As expected, *npr1-2* showed increased bacterial growth and more severe disease symptoms (Fig. 6, C and D). Another floral regulator, LFY, which acts in some of the same pathways as ANT and AIL6, also has been shown to repress responses to bacterial infection (Winter et al., 2011), suggesting that some floral transcription factors play roles in both development and defense.

Jasmonic Acid Signaling and Jasmonic Acid Levels Are Constitutively Elevated in *ant ail6* Plants

Based on the identification of the GO term jasmonic acid mediated signaling pathway (GO:0009867), we further investigated the expression of genes encoding proteins involved in jasmonic acid (JA) signaling (for review, see Pérez and Goossens, 2013). JA-Ile, the bioactive form of JA, and inositol pyrophosphate are perceived by a coreceptor complex composed of the F-box protein COI1 (a component of a SKP1-CULLIN-F-BOX-type E3 ubiquitin ligase) and a JASMONATE-ZIM DOMAIN (JAZ) protein (Fonseca et al., 2009; Yan et al., 2009; Sheard et al., 2010; Laha et al., 2015). JAZ proteins are repressors of basic helix-loop-helix MYC transcription factors, which promote JA-responsive gene expression (Chini et al., 2007). This repression occurs via the recruitment of the TOPLESS corepressor to the MYC-JAZ complex, sometimes via the adapter protein NINJA (Pauwels et al., 2010). Upon perception of JA, the JAZ proteins are ubiquitinated and targeted for destruction by the 26S proteasome, thus freeing MYCs for transcriptional activation (Thines et al., 2007). While MYC2 is the major regulator of JA-dependent gene expression, two close homologs, MYC3 and MYC4, also play roles in JA-responsive gene expression

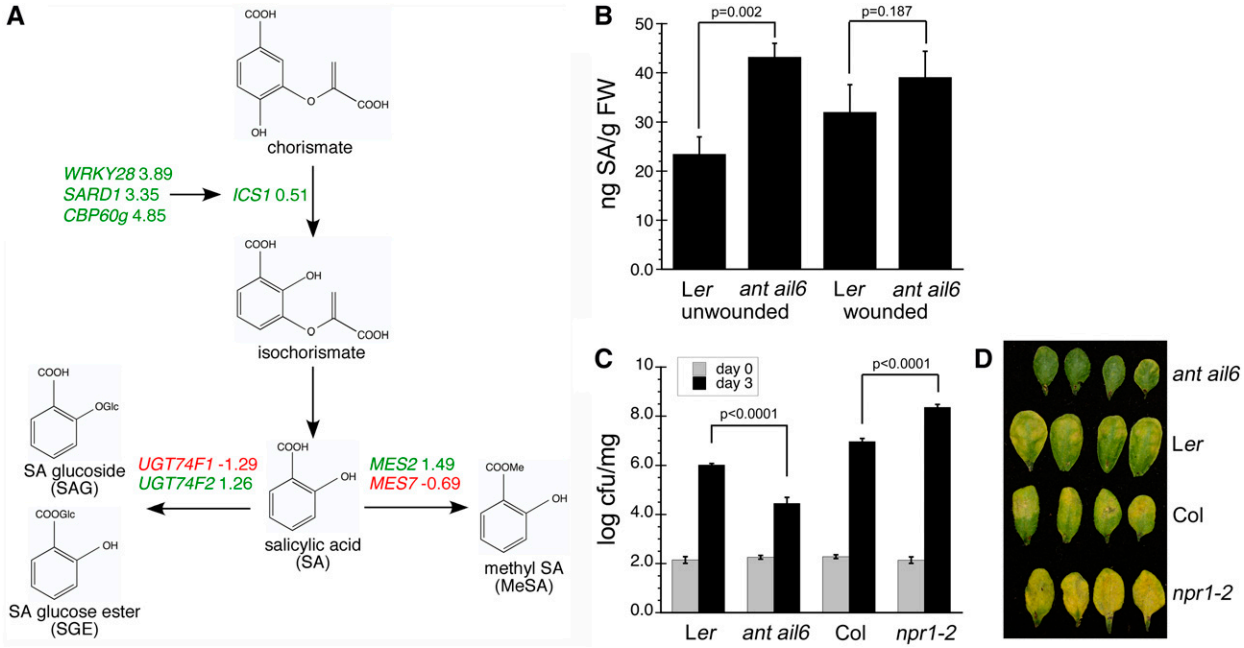

Figure 6. *ant ail6* plants have elevated SA levels and increased resistance to *P. syringae*. A, Biosynthetic and metabolic pathways that control the accumulation of SA in plants. The major SA biosynthetic pathway utilizes chorismate. A number of regulators of *ICS1* transcription, an enzyme that converts chorismate to isochorismate, are differentially expressed in *ant ail6* inflorescences. Two SA modification pathways that result in the production of SA glucoside, SA Glc ester, and methyl SA also are shown. Genes shown in red are down-regulated in *ant ail6* inflorescences, and genes shown in green are up-regulated in *ant ail6* inflorescences. The numbers beside the genes show the $\log_2$ fold change. B, SA levels are higher in unwounded *ant ail6* leaves compared with unwounded L*er* leaves. Error bars show SD, and *P* values are from Student's *t* test. FW, Fresh weight. C, Growth of *P. syringae* pv *maculicola* 4326 in L*er* and *ant ail6* at days 0 and 3 after inoculation. Columbia (Col) and *npr1-2* were used as controls. Values represent averages of five to eight plants. The error bars represent SE, and *P* values are from Student's *t* tests. The experiment was repeated three times with similar results. cfu, Colony-forming units. D, Leaves removed from plants of the indicated genotypes 3 d after infection.

(Niu et al., 2011). Several genes involved in JA signaling were identified as being differentially expressed in *ant ail6* inflorescences (Table III).

Three genes encoding negative regulators of JA signaling, *JAZ1*, *JAZ8*, and *JAZ10*, are down-regulated in *ant ail6* inflorescences, while *MYC2*, *MYC3*, and *MYC4* are up-regulated (Table III). As the JAZ family consists of 12 proteins (Chini et al., 2007), down-regulation of three *JAZ* genes may be insufficient, even in the presence of increased *MYC* expression, to promote JA signaling in *ant ail6* mutants. Therefore, to further investigate JA signaling, we examined JA-inducible gene expression in *ant ail6* inflorescences (Pauw and Memelink, 2005). A number of JA-responsive genes, including *VSP2*, *VSP1*, *JR1*, and *TAT*, are up-regulated in *ant ail6* inflorescences (Table IV). In addition, other JA-inducible genes encoding JA biosynthetic enzymes (*LOX2* and *OPR3*) and *MYC2* are up-regulated in *ant ail6* (Table III). However, members of a second class of JA-responsive genes that are synergistically induced by combined exposure to JA and ethylene (Pauw and Memelink, 2005) are either unchanged in expression (*PDF1.2*, *PR4*, *CHIB*, and *ERF1*) or down-regulated (*THI2.1*; Table IV). These results indicate that a subset of JA-responsive genes are up-regulated in *ant ail6* and suggest that these plants exhibit increased JA signaling.

JA is synthesized from α-linolenic acid through the octadecanoid pathway (Fig. 7A; for review, see Kombrink, 2012). Genes corresponding to four enzymes within the pathway are up-regulated in *ant ail6* double mutants: *LOX2*, *AOC1*, *OPR3*, and *OPCL1* (Fig. 7A; Table III), suggesting that JA levels might be increased in *ant ail6* plants. We measured JA accumulation in L*er* and *ant ail6* leaves and found higher levels in both unwounded and wounded *ant ail6* leaves compared with unwounded and wounded L*er* leaves, respectively (Fig. 7B). While JA levels are higher in *ant ail6*, *JAR1*, which encodes the enzyme that conjugates JA to Ile, is down-regulated in *ant ail6* inflorescences, so the levels of the bioactive hormone may not be elevated (Table III).

Our results suggest that both SA- and JA-signaling pathways are up-regulated in *ant ail6*. This is in contrast to the expected antagonism between these hormones. Antagonistic cross talk between SA- and JA-signaling pathways allows plants to optimize defense against a particular pest or pathogen (for review, see Thaler et al., 2012). Typically, SA mediates resistance to biotrophic pathogens while JA mediates resistance to necrotrophic

Table II. *SAR genes differentially expressed in ant ail6*

Locus	Gene	$\log_2$ Fold Change	Role in SAR
AT1G64280	*NPR1*	1.43	Nonexpressor of *PR* genes 1; transcription cofactor; master regulator of SAR
AT5G65210	*TGA1*	0.98	Transcription factor that interacts with NPR1 in SA-treated leaves
AT5G10030	*TGA4*	0.69	Transcription factor that interacts with NPR1 in SA-treated leaves
AT3G25882	*NIMIN2*	1.40	Interacts with NPR1; may be a negative regulator of SAR
AT2G14610	*PR1*	3.85	Pathogenesis-related protein 1 antimicrobial gene; unknown function
AT3G57260	*PR2*	4.32	Pathogenesis-related protein 2 antimicrobial gene; β-1,3-glucanase
AT1G75040	*PR5*	1.54	Pathogenesis-related protein 5 antimicrobial gene; thaumatin-like protein
AT4G21800	*WRKY18*	1.76	Transcription factor that promotes SAR; direct transcriptional target of NPR1
AT5G22570	*WRKY38*	4.70	Transcription factor; direct transcriptional target of NPR1
AT4G31800	*WRKY53*	0.52	Transcription factor that promotes SAR; direct transcriptional target of NPR1
AT2G40750	*WRKY54*	1.95	Transcription factor that promotes SAR; direct transcriptional target of NPR1; negative regulator of SA biosynthesis
AT3G01080	*WRKY58*	1.76	Transcription factor that blocks activation of SAR when SA levels are low
AT3G56400	*WRKY70*	1.96	Transcription factor that promotes SAR; direct transcriptional target of NPR1; negative regulator of SA biosynthesis
AT3G45640	*MPK3*	1.00	Mitogen-activated protein kinase that primes plants for SAR

pathogens and herbivorous insects. However, synergistic interactions between SA and JA also have been reported, with the nature of the interaction between these hormones being concentration dependent (Mur et al., 2006).

Identification of Direct Targets of ANT Regulation

We have identified thousands of genes that are differentially expressed in *ant ail6* compared with the wild type. This set of genes likely contains some direct targets of ANT and AIL6 regulation as well as many indirect targets. To begin to identify genes that might be direct targets of ANT regulation, we used a steroid-inducible *35S:ANT-GR* line (Yamaguchi et al., 2013). We chose several genes differentially expressed in *ant ail6* inflorescences (Fig. 8A), which were proposed previously to be directly regulated by ANT (*CYCD3;3*, *FIL*, and *YAB3*; Mizukami and Fischer, 2000; Nole-Wilson and Krizek, 2006), as well as three genes associated with auxin accumulation (*YUC2*, *TAA1*, and the auxin influx carrier *LAX3*) based on the altered auxin accumulation patterns in *ant ail6* flowers and previous work showing the direct regulation of *YUC4* by the related transcription factor AIL5 (Pinon et al., 2013). Expression of these six genes was examined in mock- and dexamethasone (DEX)-treated *35S:ANT-GR* inflorescences by RT-qPCR. No difference in expression was observed for *CYCD3;3* and *YUC2* in *35S:ANT-GR* inflorescences collected 8 h after treatment (Fig. 8, B and E). This suggests that these genes are not targets of ANT regulation and that their differential expression in *ant ail6* inflorescences is a downstream consequence of the loss of *ANT* and *AIL6* activity. We observed increased expression of *FIL*, *YAB3*, and *TAA1* after the induction of ANT activity, although the fold changes were not

Table III. *JA signaling, biosynthesis, and conjugation genes differentially expressed in ant ail6*

Locus	Gene	$\log_2$ Fold Change	Functional Role
JA signaling			
AT1G19180	*JAZ1*	−0.80	Repressor of JA signaling
AT1G30135	*JAZ8*	−1.45	Repressor of JA signaling
AT5G13220	*JAZ10*	−1.00	Repressor of JA signaling
AT1G15750	*TPL*	0.44	Corepressor that represses JA signaling
AT1G32640[a]	*MYC2*	1.01	Transcription factor that promotes JA responses
AT5G46760	*MYC3*	1.44	Transcription factor that promotes JA responses
AT4G17880	*MYC4*	1.00	Transcription factor that promotes JA responses
JA biosynthesis			
AT3G45140[a]	*LOX2*	1.00	See Figure 7
AT3G25760	*AOC1*	2.92	See Figure 7
AT2G24850[a]	*OPR3*	1.20	See Figure 7
AT1G20510	*OPCL1*	0.88	See Figure 7
JA conjugation			
AT2G46370	*JAR1*	−1.56	Catalyzes the formation of JA-Ile
AT5G07010	*ST2A*	−2.53	Catalyzes the sulfonation of 11,12-hydroxy-JA

[a]These genes are JA responsive.

Table IV. *JA-responsive gene expression in ant ail6*

Locus	Gene	$\log_2$ Fold Change	Functional Role
Changed			
AT5G24770	*VSP2*	2.46	Vegetative storage protein
AT5G24780	*VSP1*	2.04	Vegetative storage protein
AT3G16470	*JR1*	0.49	Jacalin-related lectin35
AT4G23600	*JR2*	0.72	Cys lyase
AT1G19670	*CLH1*	0.83	Chlorophyllase
AT2G24850	*TAT*	3.92	Tyr aminotransferase
AT1G72260	*THI2.1*	−1.54	Thionin
Unchanged			
AT5G44420	*PDF1.2*		Defensin; antimicrobial protein
AT3G04720	*PR4*		Hevein-like protein
AT3G12500	*CHIB*		Chitinase
AT3G23240	*ERF1*		AP2/ERF transcription factor

large (Fig. 8, C, D, and F). We also observed decreased expression of *LAX3* after the induction of ANT activity (Fig. 8G). In these four cases, the changes in gene expression in DEX-induced *35S:ANT-GR* were opposite those observed in *ant ail6* (Fig. 8, A, C, D, F, and G). To determine if these genes might be direct targets of ANT, we compared the expression of *YAB3*, *TAA1*, and *LAX3* in *35S:ANT-GR* inflorescences treated with the protein synthesis inhibitor CHX in the absence and presence of DEX. *YAB3* and *LAX3* (but not *TAA1*) exhibit similar changes in expression in the DEX+CHX-treated inflorescences, as observed in the DEX inflorescences, suggesting that they are direct targets of ANT regulation (Fig. 8, D, F, G). Furthermore, these studies suggest that ANT can act as both a transcriptional activator and a repressor.

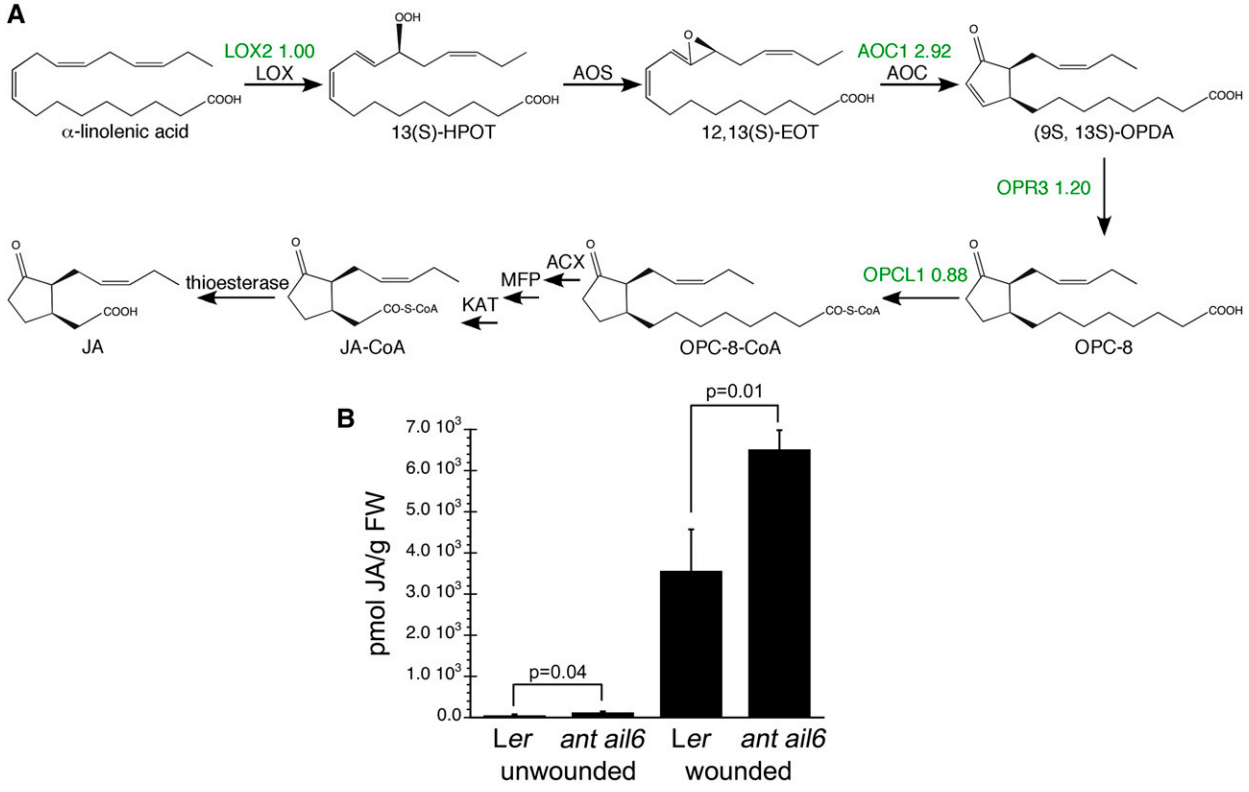

Figure 7. JA levels are higher in *ant ail6* plants. A, JA biosynthetic pathway. Genes shown in green are up-regulated in *ant ail6* inflorescences. The numbers beside the genes show the $\log_2$ fold change. B, JA levels are higher in unwounded and wounded *ant ail6* leaves compared with unwounded and wounded L*er* leaves. Error bars show SD, and *P* values are from Student's *t* tests. FW, Fresh weight. 13(S)-HPOT, 13(S)-Hydroperoxylinolenic acid; 12,13(S)-EOT, 12,13(S)-Epoxylinolenic acid; (9S,13S)-OPDA, (9S,13S) 12-oxophytodienoic acid; KAT, 3-ketoacyl-CoA-thiolase; MFP, Multifunctional protein; ACX, Acyl-CoA oxidase.

DISCUSSION

ANT and AIL6 May Regulate Floral Organ Initiation through Effects on Pectin

ANT and AIL6 contribute to the regular positioning of floral organ initiation within the flower, although how they act in this process is not known (Krizek, 2009). *ant ail6* double mutants initiate fewer floral organ primordia at relatively random positions within the flower. The results described here indicate that defects in floral organ initiation are associated with alterations in both the methylesterification status of the cell wall polysaccharide pectin and auxin accumulation patterns. A number of HG-modifying enzymes (PMEs, PMEIs, PGs, and PLLs) are differentially expressed in *ant ail6*, and levels of demethylesterified HG are reduced in young *ant ail6* flower primordia. Previous work has shown that HG undergoes demethylesterification at the sites of flower initiation within the periphery of the inflorescence meristem, with these changes both necessary and sufficient for flower primordium outgrowth (Peaucelle et al., 2008). Reduction in PME activity via transient overexpression of *PMEI3* in the inflorescence meristem of Arabidopsis plants inhibits flower primordium initiation, while transient overexpression of *PME5* results in ectopic flower formation (Peaucelle et al., 2008). Demethylesterification of HG increases tissue elasticity and likely affects cell wall extensibility to promote primordium outgrowth (Peaucelle et al., 2011). We hypothesize that a similar mechanism operates in floral meristems to promote floral organ initiation. Reduced cell wall loosening associated with high levels of methylesterified HG in *ant ail6* flower primordia may be responsible for the floral organ initiation defects present in the double mutant. It will be interesting to measure tissue elasticity in *ant ail6* flower primordia and investigate whether defects in floral organ initiation can be rescued by increased PME activity.

Auxin has been proposed to promote lateral organ outgrowth from the shoot meristem via the demethylesterification of pectin (Braybrook and Peaucelle,

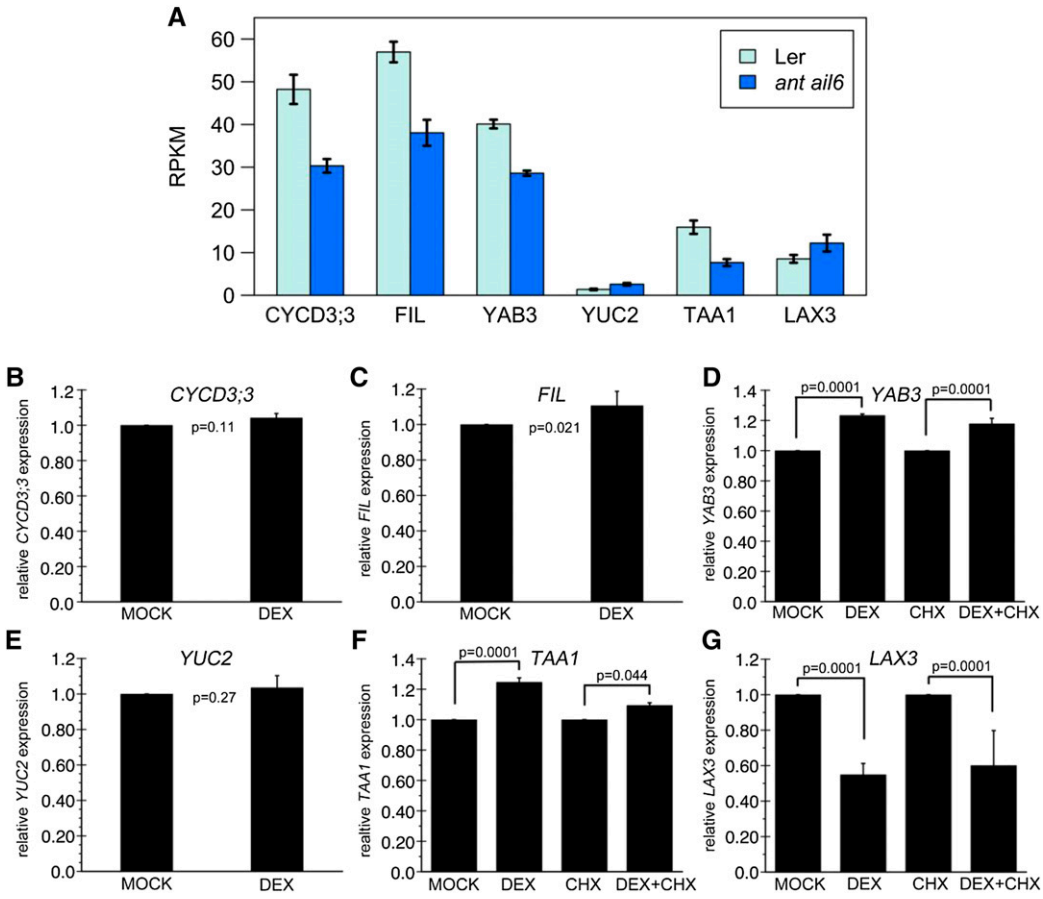

Figure 8. *YAB3* and *LAX3* may be direct targets of ANT regulation. A, Graph showing expression levels in reads per kilobase per million mapped reads (RPKM) for *CYCD3;3*, *FIL*, *YAB3*, *YUC2*, *TAA1*, and *LAX3* in L*er* and *ant ail6* inflorescences. B to G, Graphs of RT-qPCR results showing relative expression levels of *CYCD3;3* (B), *FIL* (C), *YAB3* (D), *YUC2* (E), *TAA1* (F), and *LAX3* (G) in mock- and DEX-treated or mock-, DEX-, cycloheximide (CHX)-, and DEX+CHX-treated *35S:ANT-GR* inflorescences collected 8 h after the initial treatment. The expression level in mock is set to 1, and error bars for DEX show SD; the expression level in CHX is set to 1, and error bars in DEX+CHX show SD. *P* values are from Student's *t* test.

2013). Auxin accumulates in more cells and to higher levels in *ant ail6* flower primordia, yet fewer floral organs are initiated. This suggests that ANT and AIL6 act downstream of auxin but upstream of HG demethylesterification to promote floral organ primordium outgrowth. Thus, ANT and AIL6 may mediate the induction of HG demethylesterification by auxin. Increased auxin accumulation in *ant ail6* flower primordia may be a consequence of the loss of floral organ primordia outgrowth and the concomitant creation of auxin sinks, causing auxin to pool within the flower. In the inflorescence meristem, MAP/NPY proteins, which control PIN1 localization, promote flower development by establishing a basipetal flow of auxin within incipient flower primordia that creates an auxin sink (Furutani et al., 2014). In the absence of this auxin sink, auxin accumulates throughout the surface of the inflorescence meristem and flower development does not proceed. It is not clear whether defects in auxin transport contribute to the altered pattern of auxin accumulation in young *ant ail6* flowers; *PIN1* mRNA levels are normal in *ant ail6* inflorescences. Perhaps *LAX3*, whose expression is restricted to stage 15 pedicels, petals, and stamens in wild-type flowers (Schmid et al., 2005), is ectopically expressed in young *ant ail6* flowers.

Up-Regulation of Defense Pathways in *ant ail6* Plants

Our genomic approach suggests that ANT and AIL6 repress plant defense signaling pathways and responses. In *ant ail6* mutants, we find increased levels of two plant defense hormones (SA and JA) and molecular evidence that these hormone response pathways are activated in the absence of infection. In addition, *ant ail6* plants are more resistant to the bacterial pathogen *P. syringae*. The increased resistance of *ant ail6* plants to *P. syringae* could be a consequence of constitutively activated defense pathways. In particular, three *PR* genes (*PR1*, *PR2*, and *PR5*) are up-regulated in *ant ail6* plants. Previous work has shown that constitutive expression of *PR1*, *PR2*, and *PR5* in transgenic plants overexpressing a gene encoding an acyl-CoA-binding protein, *ACBP3*, enhanced resistance of these transgenic plants to *P. syringae* (Xiao and Chye, 2011).

Additionally, the decreased methylesterification of pectin may contribute to the increased resistance of *ant ail6* plants to *P. syringae*. PMEs play important roles in the infection of plants by pathogens. To overcome the cell wall barrier during the infection process, some pathogens secrete pectin-modifying (PMEs and PMEIs) and pectin-degrading (PGs and PLLs) enzymes and induce host PME activity. Arabidopsis plants with mutations in *PME3*, a gene up-regulated upon pathogen infection, exhibit increased resistance after infection with either of two necrotrophic pathogens: the fungus *Botrytis cinerea* or the bacterium *Pectobacterium carotovorum* (Raiola et al., 2011). *pme3* mutants may be less susceptible to pathogen PGs because of their higher levels of methylesterified HG (Levesque-Tremblay et al., 2015). This suggests that a decrease in PME activity is associated with an increased resistance to necrotrophic pathogens, similar to what we have seen in *ant ail6* mutants after infection with the hemibiotroph *P. syringae*. While another study found that mutations in various *PME*s resulted in increased susceptibility to *P. syringae*, total PME activity was not decreased in these mutants, as a result of the induction of other host PMEs by the pathogen (Bethke et al., 2014).

Growth Defects of *ant ail6* Could Be a Consequence of Cell Wall Changes and/or Constitutive Defense Pathways

The growth defects of *ant ail6* double mutants (smaller rosette leaves, reduced stature, and smaller sepals) could be linked to changes in the methylesterification status of pectin and/or some other cell wall defect. Previous work has shown that reduced cell expansion contributes to the dwarf stature of *ant ail6* plants, while reduced cell number is largely responsible for the smaller leaves and sepals (Krizek, 2009). The relationship between pectin methylesterification levels and cell wall properties is complicated, making it difficult to predict how changes in HG methylesterification levels might affect cell expansion and perhaps organ growth (for review, see Levesque-Tremblay et al., 2015). PME activity can result in two distinct consequences on the cell wall: cross-linking of HG with Ca^{2+}, resulting in cell wall stiffening, or alternatively, cleavage of HG by PGs, resulting in cell wall softening. Thus, the local environment (concentration of calcium and/or PGs) is likely to play a significant role in determining the effects of PME activity on cell wall mechanical properties (for review, see Levesque-Tremblay et al., 2015). Both the degree and spatial pattern of HG methylesterification are important for determining cell wall properties. PME activity on individual GalUA residues promotes PG activity, while PME activity in a linear block-wise fashion results in stretches of free carboxylate groups that bind Ca^{2+} (Markovic and Kohn, 1984).

There are conflicting reports on the impact of HG demethylesterification on cell elongation within hypocotyls that may be a consequence of the exact pattern of methylesterification in the different experiments (for review, see Levesque-Tremblay et al., 2015). Only a few studies have reported effects of altered HG methylesterification levels on lateral organ growth. *pme3* mutants, with reduced levels of demethylesterified HG, have smaller rosettes and are slightly dwarfed (Guénin et al., 2011). However, the loss of two redundantly acting Golgi proteins (CGR2 and CGR3) that methylesterify HG results in plants with increased levels of demethylesterified HG and smaller rosette leaves (Kim et al., 2015). Thus, one cannot easily predict the consequences of changes in HG methylesterification on cell and/or organ growth.

Another possibility is that the growth defects of *ant ail6* result from constitutively activated defense pathways. A number of other Arabidopsis mutants with

constitutive disease resistance and elevated levels of SA show growth defects such as smaller rosettes and dwarf stature (Dong, 1998; Rate et al., 1999; Rate and Greenberg, 2001; Maleck et al., 2002). This demonstrates a role for SA in plant growth and development and suggests links between genes regulating plant defense and those regulating development (Rivas-San Vicente and Plasencia, 2011). In some cases, the growth defects of these mutants were partially or totally suppressed when SA levels were decreased (Rivas-San Vicente and Plasencia, 2011). It will be interesting to see if any of the growth defects of *ant ail6* double mutants are a consequence of elevated SA levels. The growth defects in *ant ail6* plants do not appear to be the consequence of a general increase in stress levels, as genes associated with abiotic stresses (cold, drought, and high salinity) are not overrepresented in the set of genes differentially expressed.

Plant survival and reproduction depend on the ability of plants to carry out growth programs while responding to biotic and abiotic stressors. The activation of costly defense responses, such as the synthesis of secondary metabolites and antimicrobial proteins, can limit resources available for plant growth and ultimately affect fitness. Thus, to optimize fitness, plants must maintain a carefully tuned balance between growth and defense responses. The ability of ANT and AIL6 to repress defense pathways may divert resources toward plant growth and development, consistent with the ability of ANT and AIL6 to promote growth during both vegetative and reproductive development (Krizek, 2009). The molecular mechanisms mediating the tradeoff between growth and defense remain largely unexplored, although they appear to involve cross talk between plant defense hormone (SA, JA, and ethylene) pathways and plant growth hormone (auxin, brassinosteroids, and GAs) pathways (Huot et al., 2014; Naseem et al., 2015). Our results suggest that ANT and AIL6 may contribute toward mechanisms regulating resource allocation between growth and defense responses to optimize fitness.

MATERIALS AND METHODS

Plant Materials and Treatments

ant-4 is in the L*er* background of Arabidopsis (*Arabidopsis thaliana*), while *ail6-2* was originally in the Columbia background. *ant-4 ail6-2* double mutants used in this study, and characterized previously (Krizek, 2009), had the *er* phenotype. Plants for the RNA-Seq and RT-qPCR experiments were grown on a soil mixture of Metro-Mix 360:perlite:vermiculite (5:1:1) in 16-h days at a light intensity of 90 μmol m^{-2} s^{-1} and temperature of 20°C. *35S:ANT-GR* is in the L*er* background (Yamaguchi et al., 2013). Inflorescences from 33-d-old *35S:ANT-GR* plants were treated twice by pipetting a mock (0.1% ethanol), 10-μm DEX, 10-μm CHX or 10-μm DEX, and 10-μm CHX solution to the inflorescences at 0 and 4 h and collected 8 h after the initial treatment.

RNA-Seq

Inflorescences were collected when the plants were 28 d old. RNA was extracted from inflorescences using Trizol following the manufacturer's instructions with cleanup on an RNeasy column (Qiagen). The RNA was DNased while on the column. Sequencing libraries (four L*er* and four *ant-4 ail6-2*) were prepared using the TruSeq RNA library preparation kit (Illumina) and sequenced on a HiSeq2000 (Illumina) using 101-base, single-end sequencing. The eight libraries were multiplexed and run twice on two lanes of an Illumina HiSeq, generating 32 to 54 million reads of 101 bp for each library. The reads were aligned onto the reference Arabidopsis genome assembly (The Arabidopsis Information Resource 10; released June 2009) using TopHat2 (Kim et al., 2013) with maximum intron size parameter set to 5,000. The number of single-mapping reads aligning to annotated Arabidopsis genes was then counted using SAMtools (Li et al., 2009). Differentially expressed genes were identified using the exactTest method in edgeR (Robinson et al., 2010) as described (Loraine et al., 2015). Genes with false discovery rates of 10^{-5} were considered differentially expressed in subsequent analyses.

RT-qPCR

RNA was isolated as described above for RNA-Seq. First-strand complementary DNA synthesis was performed using Quanta qScript cDNA SuperMix (Quanta BioSciences) following the manufacturer's instructions. Real-time PCR was performed on a Bio-Rad CFX96 using PerfeCTa SYBR Green FastMix for iQ (Quanta BioSciences) and the primers listed in Supplemental Table S2. Expression was normalized using AT5G15710 (primers RTFbox-1 and RTFbox-2; Supplemental Table S2; Czechowski et al., 2005). Data analyses were carried out as described previously (Krizek and Eaddy, 2012). The data shown are averages of two or three biological replicates. Statistical analyses were performed using Student's *t* tests on ΔCt values (Yuan et al., 2006).

Immunolocalization and in Situ Hybridization

For immunolocalization, inflorescences were fixed in FAA for 1 h, rinsed with 1× PBT, embedded, sectioned, and incubated as described previously (Jack et al., 1994). JIM5 antibody was used at a 1:10 dilution, and anti-rat IgG-FITC (Sigma-Aldrich) was used at a 1:100 dilution. The slides were counterstained with 4′,6-diamidino-2-phenylindole, mounted in Citifluor AF1, and visualized on a Leica DMI3000 fluorescence microscope. For in situ hybridization, inflorescences were fixed, embedded, sectioned, hybridized, and washed as described previously except that a hybridization temperature of 53°C was used (Krizek, 1999). The *AIL6* probe was made from a template corresponding to nucleotides 497 to 1,691 of *AIL6* that was PCR amplified with AIL6-FW2 (5′-AACTGGATCCTCGGAAGGACTCATCTTGCT-3′) and AIL6-RV2 (5′-AGGTGAATTCCCCTGAACGTTGGAGTTGTT-3′) using Phusion DNA polymerase and cloned into the *Bam*HI/*Eco*RI sites of pGEM3Z to create longAIL6/pGEM3Z. LongAIL6/pGEM3Z was linearized with *Hin*dIII and transcribed with T7 RNA polymerase. The *AIL7* probe was made from a template corresponding to nucleotides 382 to 1,402 of *AIL7* complementary DNA that was PCR amplified with AIL7-FW2 (5′-AACTGGATCCCCAGATTTCAAGACGATAAACTC-3′) and AIL7-RV2 (5′-AGGTGAATTCTCTGGTGGTAATAGAGAACTGA-3′) using Phusion DNA polymerase and cloned into the *Bam*HI/*Eco*RI sites of pGEM3Z to create longAIL7/pGEM3Z. LongAIL7/pGEM3Z was linearized with *Hin*dIII and transcribed with T7 RNA polymerase.

Confocal Microscopy

Live inflorescences were stained with FM4-64 (Invitrogen) at 10 and 1 μg mL^{-1} Silwet L-77 for the visualization of plasma membranes. After approximately 60 min, flowers were dissected from the inflorescence using a 26-gauge needle. Inflorescences were then transferred to a coverslip onto which a 24-well adhesive silicone isolator (Grace Bio-Labs) had been placed and filled with approximately 10 μL of 0.8% agarose/0.5× Murashige and Skoog salts. Confocal image stacks were acquired using a Leica TCS SP8X confocal microscope with a 40× oil-immersion lens. A 488-nm laser line was used to excite GFP, and a 640-nm laser line was used to excite FM4-64. Fluorescence was detected with a 496/533-nm (GFP) or a 640-nm (FM4-64 and chlorophyll) long-pass filter. Gain settings of 250 (GFP) and 50 (FM4-64/chlorophyll) were held constant for *DR5rev:GFP* and *DR5rev:GFP ant-4 ail6-2*. Z-stacks were collected using an average of four optical slices every 2 μm for a total of 20 μm.

SA and JA Measurements

SA and JA levels were measured using a procedure similar to one published previously (Schmelz et al., 2003). The experiment was performed twice with two to three biological replicates per experiment. The plants for these studies

were grown in short days at 22°C. Leaves were wounded with a hemostat placed perpendicular to the leaf midrib and collected 1 h after wounding. A total of 150 to 300 mg of plant tissue was homogenized in liquid nitrogen, and 100 ng of an internal standard was added. The internal standard for JA, dihydro-JA, was prepared from dihydromethyl jasmonate (Bedoukian Research) as described previously (Kandoth et al., 2007). The internal standard for SA was 2-hydroxybenzoic acid-d_6 (C/D/N Isotopes). After the addition of 600 μL of 66% (v/v) 1-propanol followed by 1,000 μL of methylene chloride, the samples were centrifuged at 3,000 rpm for 5 min and the lower methylene chloride/1-propanol phase was transferred to a 4-mL glass vial. Samples were derivatized using trimethylsilydiazomethane in hexane for 30 min at 30°C and neutralized with 2 M acetic acid in hexane for 30 min at 30°C. Volatile collection traps were made by sandwiching approximately 20 mg of Super-Q matrix (Alltech Associates) between layers of glass wool in a Pasteur pipette. The trap was inserted into the vial through a septa and connected to an air handler with a flow rate of approximately 500 to 1,000 mL min^{-1}. After drying on a heat block at 70°C with a low flow of nitrogen gas, the vial was transferred to a heating block at 200°C for an additional 1 min. Volatile compounds were eluted from the trap with 200 μL of methylene chloride. Volatiles eluted from the Super-Q matrix were analyzed by gas chromatography-mass spectrometry using electron impact ionization in selective ion mode. An HP 5890 gas chromatograph equipped with a split/splitless injector (splitless mode, injection volume of 1 mL) was interfaced to a VG-70S magnet sector mass spectrometer (Waters). Compounds were separated on a Restek RTx-5 (30 m in length, 0.25-mm i.d., and 0.2-mm film) column preheated to 80°C. After injection, the temperature was increased at 10°C min^{-1} to 130°C, then 3°C min^{-1} to 180°C, and finally 10°C min^{-1} to 300°C, and held at 300°C for 10 min. Helium was used as the carrier gas at 10 p.s.i. Specific electron impact ionization conditions were 70 eV and selection monitoring at 4,000 resolution. The retention time for SA (152.0473) was 9 min, 18 s, and that for 2-hydroxybenzoic acid-d_6 (156.0725) was 9 min, 15 s. The retention time for JA (224.1412) was 21 min, 17 s, and that for dihydro-JA (226.1569) was 21 min, 26 s.

Bacterial Growth Assay

Eighteen- to 20-d-old plants grown on a soil mixture of Metro-Mix 360:perlite: vermiculite (5:1:1) in 12-h days at a light intensity of 100 to 130 μmol m^{-2} s^{-1} and temperature of 20°C were syringe infiltrated with *Pseudomonas syringae* pv *maculicola* 4326 at an optical density at 600 nm = 0.0005. Leaf discs made using a cork borer were collected at 0 and 3 d after inoculation, and in planta bacterial growth was determined (Wang et al., 2006).

Accession Numbers

Raw sequencing data are stored at the Sequence Read Archive (http://www.ncbi.nlm.nih.gov/sra) under accession number SRP062420. Version-controlled R and python source code used to process and analyze the data are available from https://bitbucket.org/lorainelab/antail6rnaseq. Processed sequence data are available for visualization in the Integrated Genome Browser (Nicol et al., 2009) from the IGB QuickLoad site (http://www.igbquickload.org/flower).

Supplemental Data

The following supplemental materials are available.

Supplemental Figure S1. RT-qPCR on a small subset of genes identified as differentially expressed in *ant ail6* inflorescences by RNA-Seq.

Supplemental Table S1. Log_2 fold change for homogalacturonan-modifying enzymes and PMEIs differentially expressed in *ant-4 ail6-2*.

Supplemental Table S2. Primers used for RT-qPCR.

Supplemental Data S1. Genes differentially expressed in *ant ail6* inflorescences.

Supplemental Data S2. GO terms significantly enriched in genes differentially expressed in *ant ail6* inflorescences.

Supplemental Data S3. Genes associated with GO terms significantly enriched in genes differentially expressed in *ant ail6* inflorescences.

ACKNOWLEDGMENTS

We thank Jirí Friml for *DR5rev:GFP* seeds, the Complex Carbohydrate Research Center at the University of Georgia for the JIM5 antibody, Shannon Davis for help with fluorescence microscopy and use of the Leica DMI3000 fluorescence microscope, Jeff Twiss for use of the Leica TCS SP8X confocal microscope, and Mike Wang of the David H. Murdock Research Institute, who provided Illumina sequencing services.

Received October 20, 2015; accepted May 18, 2016; published May 20, 2016.

LITERATURE CITED

Benková E, Michniewicz M, Sauer M, Teichmann T, Seifertová D, Jürgens G, Friml J (2003) Local, efflux-dependent auxin gradients as a common module for plant organ formation. Cell **115:** 591–602

Bethke G, Grundman RE, Sreekanta S, Truman W, Katagiri F, Glazebrook J (2014) Arabidopsis *PECTIN METHYLESTERASE*s contribute to immunity against *Pseudomonas syringae*. Plant Physiol **164:** 1093–1107

Braybrook SA, Peaucelle A (2013) Mechano-chemical aspects of organ formation in *Arabidopsis thaliana*: the relationship between auxin and pectin. PLoS ONE **8:** e57813

Brumos J, Alonso JM, Stepanova AN (2014) Genetic aspects of auxin biosynthesis and its regulation. Physiol Plant **151:** 3–12

Cao H, Bowling SA, Gordon AS, Dong X (1994) Characterization of an *Arabidopsis* mutant that is nonresponsive to inducers of systemic acquired resistance. Plant Cell **6:** 1583–1592

Cao J (2012) The pectin lyases in *Arabidopsis thaliana*: evolution, selection and expression profiles. PLoS ONE **7:** e46944

Chandler JW, Jacobs B, Cole M, Comelli P, Werr W (2011) DORNRÖSCHEN-LIKE expression marks Arabidopsis floral organ founder cells and precedes auxin response maxima. Plant Mol Biol **76:** 171–185

Cheng Y, Dai X, Zhao Y (2006) Auxin biosynthesis by the YUCCA flavin monooxygenases controls the formation of floral organs and vascular tissues in Arabidopsis. Genes Dev **20:** 1790–1799

Chini A, Fonseca S, Fernández G, Adie B, Chico JM, Lorenzo O, García-Casado G, López-Vidriero I, Lozano FM, Ponce MR, et al (2007) The JAZ family of repressors is the missing link in jasmonate signalling. Nature **448:** 666–671

Czechowski T, Stitt M, Altmann T, Udvardi MK, Scheible WR (2005) Genome-wide identification and testing of superior reference genes for transcript normalization in Arabidopsis. Plant Physiol **139:** 5–17

Dempsey DA, Vlot AC, Wildermuth MC, Klessig DF (2011) Salicylic acid biosynthesis and metabolism. The Arabidopsis Book **9:** e0156, 10.1199/tab.0156

de Souza A, Hull PA, Gille S, Pauly M (2014) Identification and functional characterization of the distinct plant pectin esterases PAE8 and PAE9 and their deletion mutants. Planta **240:** 1123–1138

Dong X (1998) SA, JA, ethylene, and disease resistance in plants. Curr Opin Plant Biol **1:** 316–323

Ederli L, Dawe A, Pasqualini S, Quaglia M, Xiong L, Gehring C (2015) Arabidopsis flower specific defense gene expression patterns affect resistance to pathogens. Front Plant Sci **6:** 79

Fonseca S, Chini A, Hamberg M, Adie B, Porzel A, Kramell R, Miersch O, Wasternack C, Solano R (2009) (+)-7-iso-Jasmonoyl-L-isoleucine is the endogenous bioactive jasmonate. Nat Chem Biol **5:** 344–350

Friml J, Vieten A, Sauer M, Weijers D, Schwarz H, Hamann T, Offringa R, Jürgens G (2003) Efflux-dependent auxin gradients establish the apical-basal axis of Arabidopsis. Nature **426:** 147–153

Fu ZQ, Dong X (2013) Systemic acquired resistance: turning local infection into global defense. Annu Rev Plant Biol **64:** 839–863

Furutani M, Nakano Y, Tasaka M (2014) MAB4-induced auxin sink generates local auxin gradients in Arabidopsis organ formation. Proc Natl Acad Sci USA **111:** 1198–1203

Gälweiler L, Guan C, Müller A, Wisman E, Mendgen K, Yephremov A, Palme K (1998) Regulation of polar auxin transport by AtPIN1 in *Arabidopsis* vascular tissue. Science **282:** 2226–2230

Grant GT, Morris ER, Rees DA, Smith PJC, Thom D (1973) Biological interactions between polysaccharides and divalent cations: the "egg-box" model. FEBS Lett **32:** 195–198

Guénin S, Mareck A, Rayon C, Lamour R, Assoumou Ndong Y, Domon JM, Sénéchal F, Fournet F, Jamet E, Canut H, et al (2011) Identification

of pectin methylesterase 3 as a basic pectin methylesterase isoform involved in adventitious rooting in Arabidopsis thaliana. New Phytol **192:** 114–126

Heisler MG, Ohno C, Das P, Sieber P, Reddy GV, Long JA, Meyerowitz EM (2005) Patterns of auxin transport and gene expression during primordium development revealed by live imaging of the Arabidopsis inflorescence meristem. Curr Biol **15:** 1899–1911

Huot B, Yao J, Montgomery BL, He SY (2014) Growth-defense tradeoffs in plants: a balancing act to optimize fitness. Mol Plant **7:** 1267–1287

Ito T, Ng KH, Lim TS, Yu H, Meyerowitz EM (2007) The homeotic protein AGAMOUS controls late stamen development by regulating a jasmonate biosynthetic gene in *Arabidopsis*. Plant Cell **19:** 3516–3529

Ito T, Wellmer F, Yu H, Das P, Ito N, Alves-Ferreira M, Riechmann JL, Meyerowitz EM (2004) The homeotic protein AGAMOUS controls microsporogenesis by regulation of *SPOROCYTELESS*. Nature **430:** 356–360

Jack T, Fox GL, Meyerowitz EM (1994) *Arabidopsis* homeotic gene *APETALA3* ectopic expression: transcriptional and posttranscriptional regulation determine floral organ identity. Cell **76:** 703–716

Kandoth PK, Ranf S, Pancholi SS, Jayanty S, Walla MD, Miller W, Howe GA, Lincoln DE, Stratmann JW (2007) Tomato MAPKs LeMPK1, LeMPK2, and LeMPK3 function in the systemin-mediated defense response against herbivorous insects. Proc Natl Acad Sci USA **104:** 12205–12210

Kaufmann K, Wellmer F, Muiño JM, Ferrier T, Wuest SE, Kumar V, Serrano-Mislata A, Madueño F, Krajewski P, Meyerowitz EM, et al (2010) Orchestration of floral initiation by APETALA1. Science **328:** 85–89

Kim D, Pertea G, Trapnell C, Pimentel H, Kelley R, Salzberg SL (2013) TopHat2: accurate alignment of transcriptomes in the presence of insertions, deletions and gene fusions. Genome Biol **14:** R36

Kim SJ, Held MA, Zemelis S, Wilkerson C, Brandizzi F (2015) CGR2 and CGR3 have critical overlapping roles in pectin methylesterification and plant growth in *Arabidopsis thaliana*. Plant J **82:** 208–220

Knox JP, Linstead PJ, King J, Cooper C, Roberts K (1990) Pectin esterification is spatially regulated both within cell walls and between developing tissues of root apices. Planta **181:** 512–521

Kombrink E (2012) Chemical and genetic exploration of jasmonate biosynthesis and signaling paths. Planta **236:** 1351–1366

Krizek B (2009) *AINTEGUMENTA* and *AINTEGUMENTA-LIKE6* act redundantly to regulate Arabidopsis floral growth and patterning. Plant Physiol **150:** 1916–1929

Krizek BA (1999) Ectopic expression of *AINTEGUMENTA* in *Arabidopsis* plants results in increased growth of floral organs. Dev Genet **25:** 224–236

Krizek BA (2015) *AINTEGUMENTA-LIKE* genes have partly overlapping functions with *AINTEGUMENTA* but make distinct contributions to *Arabidopsis thaliana* flower development. J Exp Bot **66:** 4537–4549

Krizek BA, Eaddy M (2012) *AINTEGUMENTA-LIKE6* regulates cellular differentiation in flowers. Plant Mol Biol **78:** 199–209

Krizek BA, Fletcher JC (2005) Molecular mechanisms of flower development: an armchair guide. Nat Rev Genet **6:** 688–698

Laha D, Johnen P, Azevedo C, Dynowski M, Weiß M, Capolicchio S, Mao H, Iven T, Steenbergen M, Freyer M, et al (2015) VIH2 regulates the synthesis of inositol pyrophosphate InsP8 and jasmonate-dependent defenses in *Arabidopsis*. Plant Cell **27:** 1082–1097

Lampugnani ER, Kilinc A, Smyth DR (2013) Auxin controls petal initiation in *Arabidopsis*. Development **140:** 185–194

Levesque-Tremblay G, Pelloux J, Braybrook SA, Müller K (2015) Tuning of pectin methylesterification: consequences for cell wall biomechanics and development. Planta **242:** 791–811

Li H, Handsaker B, Wysoker A, Fennell T, Ruan J, Homer N, Marth G, Abecasis G, Durbin R (2009) The Sequence Alignment/Map format and SAMtools. Bioinformatics **25:** 2078–2079

Loraine AE, Blakley IC, Jagadeesan S, Harper J, Miller G, Firon N (2015) Analysis and visualization of RNA-Seq expression data using RStudio, Bioconductor, and Integrated Genome Browser. Methods Mol Biol **1284:** 481–501

Louvet R, Cavel E, Gutierrez L, Guénin S, Roger D, Gillet F, Guerineau F, Pelloux J (2006) Comprehensive expression profiling of the pectin methylesterase gene family during silique development in *Arabidopsis thaliana*. Planta **224:** 782–791

Maleck K, Neuenschwander U, Cade RM, Dietrich RA, Dangl JL, Ryals JA (2002) Isolation and characterization of broad-spectrum disease-resistant Arabidopsis mutants. Genetics **160:** 1661–1671

Markovic O, Kohn R (1984) Mode of pectin deesterification by Trichoderma reseei pectinesterase. Experientia **40:** 842–843

Mizukami Y, Fischer RL (2000) Plant organ size control: *AINTEGUMENTA* regulates growth and cell numbers during organogenesis. Proc Natl Acad Sci USA **97:** 942–947

Mur LA, Kenton P, Atzorn R, Miersch O, Wasternack C (2006) The outcomes of concentration-specific interactions between salicylate and jasmonate signaling include synergy, antagonism, and oxidative stress leading to cell death. Plant Physiol **140:** 249–262

Naseem M, Kaltdorf M, Dandekar T (2015) The nexus between growth and defence signalling: auxin and cytokinin modulate plant immune response pathways. J Exp Bot **66:** 4885–4896

Nicol JW, Helt GA, Blanchard SGJ Jr, Raja A, Loraine AE (2009) The Integrated Genome Browser: free software for distribution and exploration of genome-scale datasets. Bioinformatics **25:** 2730–2731

Nimchuk ZL, Zhou Y, Tarr PT, Peterson BA, Meyerowitz EM (2015) Plant stem cell maintenance by transcriptional cross-regulation of related receptor kinases. Development **142:** 1043–1049

Niu Y, Figueroa P, Browse J (2011) Characterization of JAZ-interacting bHLH transcription factors that regulate jasmonate responses in Arabidopsis. J Exp Bot **62:** 2143–2154

Nole-Wilson S, Krizek BA (2006) *AINTEGUMENTA* contributes to organ polarity and regulates growth of lateral organs in combination with *YABBY* genes. Plant Physiol **141:** 977–987

Nole-Wilson S, Tranby TL, Krizek BA (2005) *AINTEGUMENTA*-like (*AIL*) genes are expressed in young tissues and may specify meristematic or division-competent states. Plant Mol Biol **57:** 613–628

Ó'Maoiléidigh DS, Graciet E, Wellmer F (2014) Gene networks controlling *Arabidopsis thaliana* flower development. New Phytol **201:** 16–30

Ó'Maoiléidigh DS, Wuest SE, Rae L, Raganelli A, Ryan PT, Kwasniewska K, Das P, Lohan AJ, Loftus B, Graciet E, et al (2013) Control of reproductive floral organ identity specification in *Arabidopsis* by the C function regulator AGAMOUS. Plant Cell **25:** 2482–2503

Pauw B, Memelink J (2005) Jasmonate-responsive gene expression. J Plant Growth Regul **23:** 200–210

Pauwels L, Barbero GF, Geerinck J, Tilleman S, Grunewald W, Pérez AC, Chico JM, Bossche RV, Sewell J, Gil E, et al (2010) NINJA connects the co-repressor TOPLESS to jasmonate signalling. Nature **464:** 788–791

Peaucelle A, Braybrook SA, Le Guillou L, Bron E, Kuhlemeier C, Höfte H (2011) Pectin-induced changes in cell wall mechanics underlie organ initiation in *Arabidopsis*. Curr Biol **21:** 1720–1726

Peaucelle A, Louvet R, Johansen JN, Höfte H, Laufs P, Pelloux J, Mouille G (2008) *Arabidopsis* phyllotaxis is controlled by the methyl-esterification status of cell-wall pectins. Curr Biol **18:** 1943–1948

Pelloux J, Rustérucci C, Mellerowicz EJ (2007) New insights into pectin methylesterase structure and function. Trends Plant Sci **12:** 267–277

Pérez AC, Goossens A (2013) Jasmonate signalling: a copycat of auxin signalling? Plant Cell Environ **36:** 2071–2084

Pinon V, Prasad K, Grigg SP, Sanchez-Perez GF, Scheres B (2013) Local auxin biosynthesis regulation by PLETHORA transcription factors controls phyllotaxis in *Arabidopsis*. Proc Natl Acad Sci USA **110:** 1107–1112

Przemeck GK, Mattsson J, Hardtke CS, Sung ZR, Berleth T (1996) Studies on the role of the Arabidopsis gene *MONOPTEROS* in vascular development and plant cell axialization. Planta **200:** 229–237

Raiola A, Lionetti V, Elmaghraby I, Immerzeel P, Mellerowicz EJ, Salvi G, Cervone F, Bellincampi D (2011) Pectin methylesterase is induced in Arabidopsis upon infection and is necessary for a successful colonization by necrotrophic pathogens. Mol Plant Microbe Interact **24:** 432–440

Randall RS, Sornay E, Dewitte W, Murray JA (2015) AINTEGUMENTA and the D-type cyclin CYCD3;1 independently contribute to petal size control in Arabidopsis: evidence for organ size compensation being an emergent rather than a determined property. J Exp Bot **66:** 3991–4000

Rate DN, Cuenca JV, Bowman GR, Guttman DS, Greenberg JT (1999) The gain-of-function *Arabidopsis acd6* mutant reveals novel regulation and function of the salicylic acid signaling pathway in controlling cell death, defenses, and cell growth. Plant Cell **11:** 1695–1708

Rate DN, Greenberg JT (2001) The *Arabidopsis aberrant growth and death2* mutant shows resistance to *Pseudomonas syringae* and reveals a role for NPR1 in suppressing hypersensitive cell death. Plant J **27:** 203–211

Reinhardt D, Pesce ER, Stieger P, Mandel T, Baltensperger K, Bennett M, Traas J, Friml J, Kuhlemeier C (2003) Regulation of phyllotaxis by polar auxin transport. Nature **426:** 255–260

Rivas-San Vicente M, Plasencia J (2011) Salicylic acid beyond defence: its role in plant growth and development. J Exp Bot **62:** 3321–3338

Robinson MD, McCarthy DJ, Smyth GK (2010) edgeR: a Bioconductor package for differential expression analysis of digital gene expression data. Bioinformatics **26:** 139–140

Schmelz EA, Engelberth J, Alborn HT, O'Donnell P, Sammons M, Toshima H, Tumlinson JHI III (2003) Simultaneous analysis of phytohormones, phytotoxins, and volatile organic compounds in plants. Proc Natl Acad Sci USA **100:** 10552–10557

Schmid M, Davison TS, Henz SR, Pape UJ, Demar M, Vingron M, Schölkopf B, Weigel D, Lohmann JU (2005) A gene expression map of Arabidopsis thaliana development. Nat Genet **37:** 501–506

Sénéchal F, Wattier C, Rustérucci C, Pelloux J (2014) Homogalacturonan-modifying enzymes: structure, expression, and roles in plants. J Exp Bot **65:** 5125–5160

Sheard LB, Tan X, Mao H, Withers J, Ben-Nissan G, Hinds TR, Kobayashi Y, Hsu FF, Sharon M, Browse J, et al (2010) Jasmonate perception by inositol-phosphate-potentiated COI1-JAZ co-receptor. Nature **468:** 400–405

Sun L, van Nocker S (2010) Analysis of promoter activity of members of the *PECTATE LYASE-LIKE* (*PLL*) gene family in cell separation in Arabidopsis. BMC Plant Biol **10:** 152

Thaler JS, Humphrey PT, Whiteman NK (2012) Evolution of jasmonate and salicylate signal crosstalk. Trends Plant Sci **17:** 260–270

Thines B, Katsir L, Melotto M, Niu Y, Mandaokar A, Liu G, Nomura K, He SY, Howe GA, Browse J (2007) JAZ repressor proteins are targets of the SCF(COI1) complex during jasmonate signalling. Nature **448:** 661–665

Vieten A, Vanneste S, Wisniewska J, Benková E, Benjamins R, Beeckman T, Luschnig C, Friml J (2005) Functional redundancy of PIN proteins is accompanied by auxin-dependent cross-regulation of PIN expression. Development **132:** 4521–4531

Wang D, Amornsiripanitch N, Dong X (2006) A genomic approach to identify regulatory nodes in the transcriptional network of systemic acquired resistance in plants. PLoS Pathog **2:** e123

Wang M, Yuan D, Gao W, Li Y, Tan J, Zhang X (2013) A comparative genome analysis of PME and PMEI families reveals the evolution of pectin metabolism in plant cell walls. PLoS ONE **8:** e72082

Winter CM, Austin RS, Blanvillain-Baufumé S, Reback MA, Monniaux M, Wu MF, Sang Y, Yamaguchi A, Yamaguchi N, Parker JE, et al (2011) LEAFY target genes reveal floral regulatory logic, *cis* motifs, and a link to biotic stimulus response. Dev Cell **20:** 430–443

Wuest SE, O'Maoileidigh DS, Rae L, Kwasniewska K, Raganelli A, Hanczaryk K, Lohan AJ, Loftus B, Graciet E, Wellmer F (2012) Molecular basis for the specification of floral organs by APETALA3 and PISTILLATA. Proc Natl Acad Sci USA **109:** 13452–13457

Xiao S, Chye ML (2011) Overexpression of Arabidopsis ACBP3 enhances NPR1-dependent plant resistance to *Pseudomonas syringe* pv *tomato* DC3000. Plant Physiol **156:** 2069–2081

Yamaguchi N, Wu MF, Winter CM, Berns MC, Nole-Wilson S, Yamaguchi A, Coupland G, Krizek BA, Wagner D (2013) A molecular framework for auxin-mediated initiation of flower primordia. Dev Cell **24:** 271–282

Yan J, Zhang C, Gu M, Bai Z, Zhang W, Qi T, Cheng Z, Peng W, Luo H, Nan F, et al (2009) The *Arabidopsis* CORONATINE INSENSITIVE1 protein is a jasmonate receptor. Plant Cell **21:** 2220–2236

Yuan JS, Reed A, Chen F, Stewart CNJ Jr (2006) Statistical analysis of real-time PCR data. BMC Bioinformatics **7:** 85

Zhang P, Foerster H, Tissier CP, Mueller L, Paley S, Karp PD, Rhee SY (2005) MetaCyc and AraCyc: metabolic pathway databases for plant research. Plant Physiol **138:** 27–37